Journal of Quantitative Spectroscopy & Radiative Transfer 111 (2010) 214–225

Contents lists available at ScienceDirect

Journal of Quantitative Spectroscopy & Radiative Transfer

journal homepage: www.elsevier.com/locate/jqsrt

One-dimensional photonic crystal design

Cornelis van der Mee [a,*], Pietro Contu [a], Paolo Pintus [b]

[a] Dipartimento di Matematica e Informatica, Università degli Studi di Cagliari, Viale Merello 92, 09123 Cagliari, Italy
[b] CEIIC, Scuola Superiore di Studi Universitari e Perfezionamento Sant'Anna, Via G. Moruzzi 1, 56124 Pisa, Italy

ARTICLE INFO

Article history:
Received 6 April 2009
Received in revised form
9 July 2009
Accepted 10 July 2009

Keywords:
Photonic crystal
Maxwell's equations
Helmholtz equation
Period map
Scattering matrix
Impurity period map

ABSTRACT

In this article we present a method to determine the band spectrum, band gaps, and discrete energy levels, of a one-dimensional photonic crystal with localized impurities. For one-dimensional crystals with piecewise constant refractive indices we develop an algorithm to recover the refractive index distribution from the period map. Finally, we derive the relationship between the period map and the scattering matrix containing the information on the localized modes.

1. Introduction

Photonic crystals are nanostructures in which, as in a semiconductor crystal, the periodic variation of its physical properties, i.e. its electric permittivity or, equivalently, its refractive index, leads to photonic bands of frequencies at which light can travel and be scattered, and photonic band gaps of frequencies at which light cannot pass. This kind of crystal may be observed in nature in the frustules of some unicellular algae (diatoms) [1] or on the surface of butterfly wings [2]. The band structure is also the reason of some unusual optical properties such as diffractive reflection and refraction, supercollimation, and the superprism effect [3].

Introducing a disorder in the periodic dielectric structure by doping the crystal with an impurity or by locally altering the crystal periodicity, does not affect the band structure of the electromagnetic spectrum, but may create localized modes within band gaps at which stationary waves may occur [4,5].

The main purpose of photonic crystal modeling is the design of devices with prescribed spectral properties such as allowed and forbidden frequency intervals, based on the identification of the spatial refractive index variation using constraints on the frequency spectrum. Nowadays it is possible to design photonic crystal fibers [6,7] introducing impurities allowing us to confine light (resonant cavities and laser Fabry–Perot cavities [8]) or to create preferred pathways to guide it (waveguides) [9–11].

Standard optical fibers rely on light being guided by the physical law known as *total internal reflection* (TIR) or *index guiding*. In order to achieve TIR in these fibers, which are formed from dielectrics or semiconductors, it is necessary that the refractive index of the core exceeds that of the surrounding media. In photonic crystal fibers light is constrained to propagate along photonic band gaps, while the core is a different medium with a smaller refractive index. These fibers have properties important to telecommunication that differ from those of standard fibers: they allow bending by larger angles and light dissipation is much more negligible.

Other important applications are multiplexing, demultiplexing and switching. Using negative refraction, supercollimation and the superprism effect, an optical demultiplexer has been designed by a research group at the

* Corresponding author. Tel.: +39 70 6755605; fax: +39 70 6755601.
E-mail addresses: cornelis@unica.it (C. van der Mee), contu22@interfree.it (P. Contu), paolo.pintus@sssup.it (P. Pintus).

0022-4073/$ - see front matter © 2009 Elsevier Ltd. All rights reserved.
doi:10.1016/j.jqsrt.2009.07.003

Georgia Institute of Technology [12], while the Kerr effect permits one to design basic components of integrated optics like optical transistors [13].

A fundamental problem in this field is the design of a photonic crystal with specified properties; engineering design is formally a type of mathematical Inverse Problem: given the allowed frequencies and the photonic path at each allowed frequency, what is the corresponding refractive index as a function of the location in the crystal? In the literature the Level Set Method [14,15] has emerged as an excellent tool that can contribute to algorithms for the optimization of boundaries and edges. A successful design method for photonic crystals will have a big impact in computer circuitry. The replacement of the electric current with a photonic flow will enable us to build future optical integrated circuits that are much faster, use much less energy, and dissipate much less heat.

In this paper we deal with one-dimensional photonic crystals where, except for impurity variations, the refractive index is periodic in the direction of propagation of the light. In the purely periodic case there have traditionally been two methods to compute the bands and band gaps, namely the transfer matrix method [16,17] and the plane wave expansion method [18,5]. In this article, as in [19,20], we apply the spectral theory of Hill's equation [21–23], modified to be applicable to Helmholtz's equation with periodic boundary conditions, to compute the bands and band gaps as those frequency intervals where the so-called Hill discriminant is smaller or larger than 2 in absolute value, respectively. This Hill discriminant appears as the trace of a real 2×2 matrix, the period map, which relates the initial data of the solution of Helmholtz's equation at the right endpoint of a period to those at a left endpoint. Contrary to [19,20], we do not derive conditions for having empty band gaps. For one-dimensional crystals composed of finitely many different materials with constant refractive index, which is a suitable model for describing heterojunctions such as AlGa–AlAs or InAs–AlSb, we compute the Hill discriminant and hence the band spectrum in closed form. Conversely, in this "piecewise constant" case we evaluate the refractive index as a function of position from the spectral data in two steps:

1. We develop a method to recover the refractive index of such material as a function of position from the period map for one period. This period may have the same material composition as the periodic crystal or may contain the impurities.
2. We describe a method to evaluate the period map from the scattering matrix containing the information on the localized modes.

This method allows us, in principle, to reconstruct a one-dimensional crystal consisting of finitely many materials with constant refractive index from the band spectrum and the scattering matrix, provided the impurities, now consisting of a modified arrangement of the material layers, are confined to one period.

2. Physical and mathematical model

The propagation of light in a photonic crystal is described by Maxwell's equations. Let $\boldsymbol{E}(\boldsymbol{r},t)$ and $\boldsymbol{H}(\boldsymbol{r},t)$ stand for the electric and magnetic fields, and $\boldsymbol{D}(\boldsymbol{r},t)$ and $\boldsymbol{B}(\boldsymbol{r},t)$ for the displacement and magnetic induction fields, as a function of position $\boldsymbol{r}$ and time t. Assume photonic crystals to be linear, isotropic, magnetically homogeneous, and lossless materials without free charges and current densities, so that

$$\boldsymbol{D}(\boldsymbol{r},t)=\varepsilon_0\varepsilon(\boldsymbol{r})\boldsymbol{E}(\boldsymbol{r},t),\quad \boldsymbol{B}(\boldsymbol{r},t)=\mu_0\mu\boldsymbol{H}(\boldsymbol{r},t), \tag{2.1}$$

where the electric permittivity $\varepsilon(\boldsymbol{r})$ is real-valued. Limiting ourselves to harmonic modes,

$$\boldsymbol{H}(\boldsymbol{r},t)=\boldsymbol{H}(\boldsymbol{r})e^{i\omega t},\quad \boldsymbol{E}(\boldsymbol{r},t)=\boldsymbol{E}(\boldsymbol{r})e^{i\omega t}, \tag{2.2}$$

Maxwell's equations become

$$\nabla\times\boldsymbol{H}(\boldsymbol{r})=-i\omega\varepsilon_0\varepsilon(\boldsymbol{r})\boldsymbol{E}(\boldsymbol{r}), \tag{2.3}$$

$$\nabla\times\boldsymbol{E}(\boldsymbol{r})=i\omega\mu_0\mu\boldsymbol{H}(\boldsymbol{r}), \tag{2.4}$$

$$\nabla\cdot(\varepsilon(\boldsymbol{r})\boldsymbol{E}(\boldsymbol{r}))=0, \tag{2.5}$$

$$\nabla\cdot(\mu\boldsymbol{H}(\boldsymbol{r}))=0, \tag{2.6}$$

which can be decoupled as follows:

$$\frac{1}{\mu}\nabla\times[\nabla\times\boldsymbol{E}(\boldsymbol{r})]=\eta\varepsilon(\boldsymbol{r})\boldsymbol{E}(\boldsymbol{r}), \tag{2.7}$$

$$\nabla\cdot[\varepsilon(\boldsymbol{r})\boldsymbol{E}(\boldsymbol{r})]=0, \tag{2.8}$$

$$\nabla\times\left[\frac{1}{\varepsilon(\boldsymbol{r})}\nabla\times\boldsymbol{H}(\boldsymbol{r})\right]=\eta\mu\boldsymbol{H}(\boldsymbol{r}), \tag{2.9}$$

$$\nabla\cdot[\mu\boldsymbol{H}(\boldsymbol{r})]=0, \tag{2.10}$$

where μ is the constant magnetic permeability and $\eta\stackrel{\text{def}}{=}\omega^2/c^2$ serves as the spectral parameter. Let $n(\boldsymbol{r})=\sqrt{\varepsilon(\boldsymbol{r})\mu}$ denote the refractive index.

Focusing on a one-dimensional pure photonic crystal, if we consider TEM modes, i.e., polarized light propagating along the periodic direction and $\boldsymbol{E}$ and $\boldsymbol{H}$ parallel to the yz plane (Fig. 1), it is straightforward to see that the electric eigenvalue problem (2.7)–(2.8) turns into the Helmholtz equation:

$$-\psi''(\eta,x)=\eta n^2(x)\psi(\eta,x), \tag{2.11}$$

where $x\in\mathbb{R}$, the prime denotes differentiation with respect to x, the refractive index $n(x)$ is a periodic function with period $p>0$, i.e., $n(x+p)\equiv n(x)$, and $\psi(\eta,x)$ is the polarized component of the electric field.

3. Hill discriminant and period map

The spectral theory of Hill's equation (i.e., the one-dimensional Schrödinger equation with periodic boundary conditions) is well developed [21–23] and can obviously be applied to describe one-dimensional solids and semiconductors without impurities. In this section we give the theoretical background on the one-dimensional Helmholtz equation with periodic boundary conditions [i.e. Eq. (2.11)] to describe a one-dimensional photonic

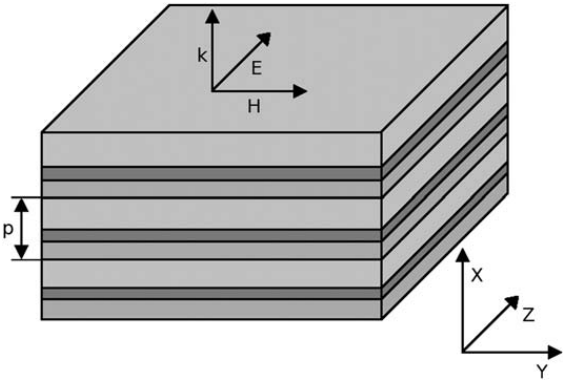

Fig. 1. In a one-dimensional pure photonic crystal the dielectric medium is periodic only in one direction (x-axis). Polarized light propagates along the x-axis, while the magnetic field H and the electric field E are directed along the y- and z-axes, respectively, and depend only on the x-variable (TEM modes).

crystal without impurities. For the proofs, which closely mimic those for Hill's equation, we refer to [21–23].

There exist unique linearly independent solutions $\theta(\eta,x)$ and $\varphi(\eta,x)$ of Eq. (2.11), called elementary solutions, satisfying the initial conditions

$$\theta(\eta,0)=1, \quad \theta'(\eta,0)=0, \tag{3.1a}$$

$$\varphi(\eta,0)=0, \quad \varphi'(\eta,0)=1. \tag{3.1b}$$

Now assume $\psi(x)\not\equiv 0$ is a solution of Eq. (2.11) satisfying the τ-periodic or Born–Von Kármán conditions

$$\psi(\eta,p)=\tau\psi(\eta,0), \tag{3.2a}$$

$$\psi'(\eta,p)=\tau\psi'(\eta,0), \tag{3.2b}$$

for some constant $0\neq\tau\in\mathbb{C}$. Let us write the general solution $\psi(\eta,x)$ of Eq. (2.11) satisfying conditions (3.2) as a linear combination of the elementary solutions $\theta(\eta,x)$ and $\varphi(\eta,x)$. Then the linear combination

$$c_1\theta(\eta,x)+c_2\varphi(\eta,x)$$

satisfies the boundary conditions (3.2) if and only if the linear system

$$\begin{pmatrix} \tau-\theta(\eta,p) & -\varphi(\eta,p) \\ -\theta'(\eta,p) & \tau-\varphi'(\eta,p) \end{pmatrix}\begin{pmatrix} c_1 \\ c_2 \end{pmatrix}=\begin{pmatrix} 0 \\ 0 \end{pmatrix}$$

has a non-trivial solution, i.e., if and only if the system determinant

$$\tau^2-[\theta(\eta,p)+\varphi'(\eta,p)]\tau+1 \tag{3.3}$$

vanishes. Note that the Wronskian $w=\theta\varphi'-\theta'\varphi=1$.

The fundamental matrix of Eq. (2.11) evaluated at $x=p$ is referred to as the *period map*

$$\boldsymbol{M}(\eta)\stackrel{\text{def}}{=}\begin{pmatrix} \theta(\eta,p) & \varphi(\eta,p) \\ \theta'(\eta,p) & \varphi'(\eta,p) \end{pmatrix}, \tag{3.4}$$

and its trace

$$\Delta(\eta)=\theta(\eta,p)+\varphi'(\eta,p), \tag{3.5}$$

is the *Hill discriminant*. Making use of condition (3.3), we have

$$\tau^2-\Delta(\eta)\tau+1=0, \tag{3.6}$$

which implies that

$$\tau_1\tau_2=1, \quad \tau_1+\tau_2=\Delta(\eta), \tag{3.7}$$

being τ_1 and τ_2 the roots of Eq. (3.6). As a result, from (3.7) we get

$$\Delta(\eta)=\tau+\tau^{-1}, \tag{3.8}$$

where τ is a root of Eq. (3.6). Generalizing the Born–Von Kármán condition to m periods we get

$$\psi(\eta,x+mp)=\tau^m\psi(\eta,x), \tag{3.9}$$

from which we can easily see that solutions $\psi\neq 0$ satisfying (3.2), are unbounded as $x\to+\infty$ if $|\tau|>1$ and as $x\to-\infty$ if $|\tau|<1$. Therefore the boundedness of such solutions ψ requires $|\tau|=1$. We thus arrive at the Bloch representation

$$\psi(\eta,x)=e^{ik(\eta)y(x)}\chi(\eta,x),$$

where $y(x)=\int_0^x n(\hat{x})\,d\hat{x}$ is a travel time parameter, $k(\eta)$ is the quasi-momentum to be discussed shortly, and $\chi(\eta,x)$ is periodic in x with period p. Moreover, Hill's discriminant becomes

$$\Delta(\eta)=\tau_1+\tau_1^{-1}=e^{ikq}+e^{-ikq}=2\cos(kq), \tag{3.10}$$

where $q=y(p)$ is the travel time in one period. Hence [22, Chapter XXI, 21,23] there exist bounded solutions if and only if $\Delta(\eta)\in[-2,2]$. Outside this range there is no physical solution, because the corresponding waves would have infinite energy.

In the sequel we shall write many quantities in terms of the quasimomentum k which is given in terms of η and the one-period travel time q by Firsova's Formula [25]

$$k(\eta)=\frac{1}{q}\arcsin\left(\frac{i}{2}\sqrt{\Delta(\eta)^2-4}\right). \tag{3.11}$$

Formula (3.11) defines a conformal mapping from the complex η-plane cut along the bands onto the upper half complex k-plane, where the bands approached from above correspond to the positive real k-line and the bands approached from below to the negative real k-line. When writing (2.11) in the travel time parameter, under conditions of sufficient smoothness on the refractive index $n(x)$ one can write (2.11) as Hill's equation in the new position variable y, where the part of momentum is now played by the quasimomentum. In particular, if $n(x)\equiv 1$, we have $q=p$ and $k(\eta)=i\sqrt{-\eta}$, which is the usual momentum.

For the homogeneous medium where $n(x)=n>0$, we have

$$\theta(\eta,x;n)=\cos(n\sqrt{\eta}x), \quad \varphi(\eta,x;n)=\frac{\sin(n\sqrt{\eta}x)}{n\sqrt{\eta}},$$

so that

$$\Delta(\eta;n)=2\cos(n\sqrt{\eta}p). \tag{3.12}$$

Then the zeros $\{\eta_j\}_{j=0}^{\infty}$ of $\Delta(\eta;n)=2$ and $\{\tilde{\eta}_j\}_{j=1}^{\infty}$ of $\Delta(\eta;n)=-2$ are given by

$$\eta_j=\begin{cases}\left(\dfrac{j\pi}{np}\right)^2, & j \text{ even},\\ \left(\dfrac{(j+1)\pi}{np}\right)^2, & j \text{ odd},\end{cases}$$

$$\tilde{\eta}_j=\begin{cases}\left(\dfrac{(j-1)\pi}{np}\right)^2, & j \text{ even},\\ \left(\dfrac{j\pi}{np}\right)^2, & j \text{ odd}.\end{cases}$$

Thus (the interiors of) the bands are

$$\left(\left[\frac{(j-1)\pi}{np}\right]^2,\left[\frac{j\pi}{np}\right]^2\right),\quad j=1,2,3,\ldots,$$

whereas the band gaps are empty.

4. Piecewise constant refractive index

The piecewise constant case perfectly fits the description of a one-dimensional photonic crystal, i.e. regular arrays of different dielectric materials layered along one spatial direction as displayed in Fig. 2. We then have $n(x)=n_j$ $(b_{j-1}<x<b_j,\ j=1,\ldots,m)$, where $0=b_0<b_1<\cdots<b_m=p$ and $a_j=b_j-b_{j-1}$ $(j=1,\ldots,m)$. Then any solution $\psi_j(\eta,x)$ of (2.11) on (b_{j-1},b_j) satisfies

$$\psi_j(\eta,x)=c_{1j}\theta(\eta,x-b_{j-1};n_j)+c_{2j}\varphi(\eta,x-b_{j-1};n_j), \tag{4.1a}$$

$$\psi_j'(\eta,x)=-(n_j\sqrt{\eta})^2c_{1j}\varphi(\eta,x-b_{j-1};n_j)+c_{2j}\theta(\eta,x-b_{j-1};n_j), \tag{4.1b}$$

where $j=1,\ldots,m$. The requirement that $\psi(\eta,x)$ is continuously differentiable at the points $b_1,\ldots,b_{m-1}$ leads to the identities

$$\begin{pmatrix}c_{1j}\\ c_{2j}\end{pmatrix}=\boldsymbol{A}_{j-1}(\eta)\begin{pmatrix}c_{1,j-1}\\ c_{2,j-1}\end{pmatrix},\quad j=2,\ldots,m,$$

where

$$\boldsymbol{A}_{j-1}(\eta)=\begin{pmatrix}\theta(\eta,a_{j-1};n_{j-1}) & \varphi(\eta,a_{j-1};n_{j-1})\\ -(n_{j-1}\sqrt{\eta})^2\varphi(\eta,a_{j-1};n_{j-1}) & \theta(\eta,a_{j-1};n_{j-1})\end{pmatrix}.$$

Thus

$$\begin{pmatrix}c_{1m}\\ c_{2m}\end{pmatrix}=\boldsymbol{A}_{m-1}(\eta)\ldots\boldsymbol{A}_2(\eta)\boldsymbol{A}_1(\eta)\begin{pmatrix}c_{11}\\ c_{21}\end{pmatrix}.$$

On the other hand,

$$\begin{pmatrix}\psi(\eta,p)\\ \psi'(\eta,p)\end{pmatrix}=\boldsymbol{A}_m(\eta)\begin{pmatrix}c_{1m}\\ c_{2m}\end{pmatrix}.$$

Consequently,

$$\begin{pmatrix}\psi(\eta,p)\\ \psi'(\eta,p)\end{pmatrix}=\boldsymbol{M}(\eta)\begin{pmatrix}\psi(\eta,0)\\ \psi'(\eta,0)\end{pmatrix},$$

where the period map $\boldsymbol{M}(\eta)$ is defined by

$$\boldsymbol{M}(\eta)=\boldsymbol{A}_m(\eta)\boldsymbol{A}_{m-1}(\eta)\ldots\boldsymbol{A}_2(\eta)\boldsymbol{A}_1(\eta). \tag{4.2}$$

Having $\psi=\theta$ and $\psi=\varphi$, respectively, and using (3.1) we get

$$\boldsymbol{M}(\eta)=\begin{pmatrix}\theta(\eta,p) & \varphi(\eta,p)\\ \theta'(\eta,p) & \varphi'(\eta,p)\end{pmatrix}. \tag{4.3}$$

Hence the Hill discriminant is given by

$$\Delta(\eta)=\mathrm{Tr}[\boldsymbol{M}(\eta)]=\theta(\eta,p)+\varphi'(\eta,p). \tag{4.4}$$

In various special cases the function $\Delta(\eta)$ allows us to evaluate the crystal's band structure (Fig. 3). For $m=2$ we get

$$\Delta(\eta)=2\Big[\cos(n_2a_2\sqrt{\eta})\cos(n_1a_1\sqrt{\eta})-\frac{1}{2}\left(\frac{n_1}{n_2}+\frac{n_2}{n_1}\right)\sin(n_2a_2\sqrt{\eta})\sin(n_1a_1\sqrt{\eta})\Big]. \tag{4.5}$$

For $m=3$ we get

$$\begin{aligned}\Delta(\eta)=2\Big[&\cos(n_3a_3\sqrt{\eta})\cos(n_2a_2\sqrt{\eta})\cos(n_1a_1\sqrt{\eta})\\ &-\frac{1}{2}\left(\frac{n_1}{n_2}+\frac{n_2}{n_1}\right)\cos(n_3a_3\sqrt{\eta})\sin(n_2a_2\sqrt{\eta})\sin(n_1a_1\sqrt{\eta})\\ &-\frac{1}{2}\left(\frac{n_1}{n_3}+\frac{n_3}{n_1}\right)\sin(n_3a_3\sqrt{\eta})\cos(n_2a_2\sqrt{\eta})\sin(n_1a_1\sqrt{\eta})\\ &-\frac{1}{2}\left(\frac{n_2}{n_3}+\frac{n_3}{n_2}\right)\sin(n_3a_3\sqrt{\eta})\sin(n_2a_2\sqrt{\eta})\cos(n_1a_1\sqrt{\eta})\Big].\end{aligned}$$

In general, the period map $\boldsymbol{M}(\eta)$ has the form

$$\boldsymbol{M}(\eta)=\prod_{j=m,m-1,\ldots,1}\begin{pmatrix}\cos(n_ja_j\sqrt{\eta}) & \dfrac{\sin(n_ja_j\sqrt{\eta})}{n_j\sqrt{\eta}}\\ -n_j\sqrt{\eta}\sin(n_ja_j\sqrt{\eta}) & \cos(n_ja_j\sqrt{\eta})\end{pmatrix},$$

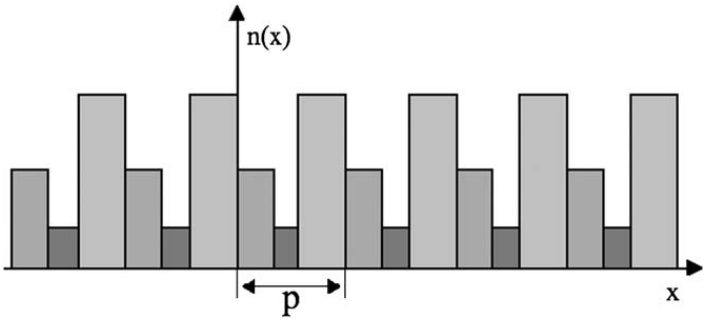

Fig. 2. Example of a periodic structure with period p in the case of a piecewise constant refractive index. The figure illustrates a one-dimensional three layer photonic crystal with different layer amplitudes.

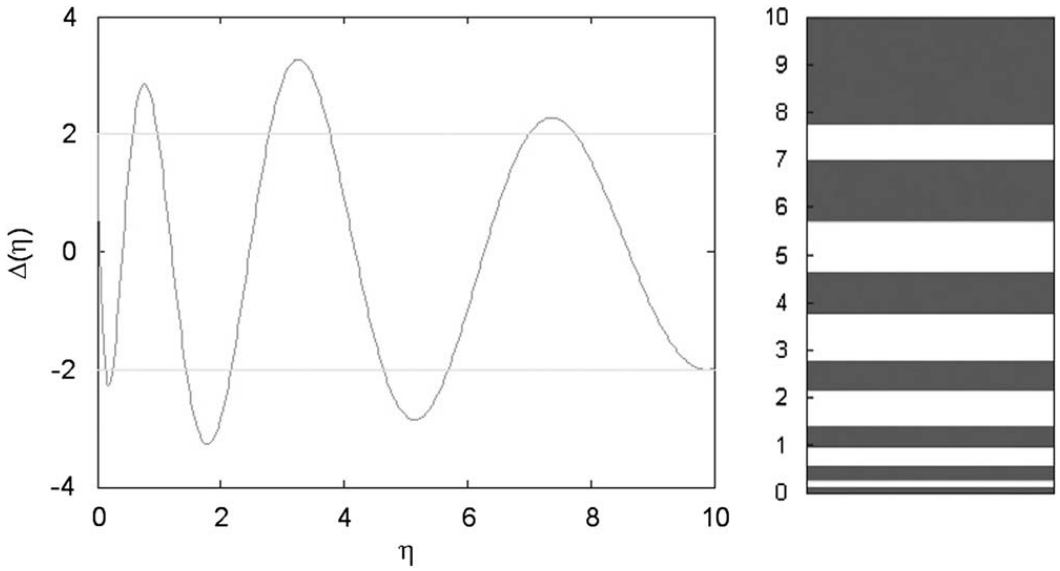

Fig. 3. Graph of $\Delta(\eta)$ as a function of $\sqrt{\eta}$ for a three layer photonic crystal ($m=3$), where $n_1=1.5$, $n_2=1$, $n_3=2$, $a_1=1$, $a_2=2$, and $a_3=0.8$. On the right the allowed bands are displayed in dark and white.

which implies

$$\lim_{\eta\to 0^+}\boldsymbol{M}(\eta)=\prod_{j=m,m-1,\ldots,1}\begin{pmatrix}1 & a_j\\ 0 & 1\end{pmatrix}=\begin{pmatrix}1 & a_1+\cdots+a_m\\ 0 & 1\end{pmatrix}. \tag{4.6}$$

Therefore the crystal period p equals the non-diagonal entry $M^{12}(\eta)$ of the period map as $\eta\to 0^+$. Moreover, we easily see that

$$\begin{pmatrix}\sqrt{\eta} & 0\\ 0 & 1\end{pmatrix}\boldsymbol{M}(\eta)\begin{pmatrix}\frac{1}{\sqrt{\eta}} & 0\\ 0 & 1\end{pmatrix}=\prod_{j=m,m-1,\ldots,1}\begin{pmatrix}\cos(n_ja_j\sqrt{\eta}) & \dfrac{\sin(n_ja_j\sqrt{\eta})}{n_j}\\ -n_j\sin(n_ja_j\sqrt{\eta}) & \cos(n_ja_j\sqrt{\eta})\end{pmatrix}, \tag{4.7}$$

where the right-hand side is called *modified period map*, has determinant 1 and whose entries are almost periodic polynomials in $\sqrt{\eta}$. The diagonal entries are real even functions of $\sqrt{\eta}$ and the off-diagonal entries are real odd functions of $\sqrt{\eta}$ vanishing at $\sqrt{\eta}=0$.

Let us write

$$\mu_j=n_ja_j>0,\quad z=\sqrt{\eta},$$
$$\mathbb{M}(z)=\begin{pmatrix}z & 0\\ 0 & 1\end{pmatrix}\boldsymbol{M}(\eta)\begin{pmatrix}z^{-1} & 0\\ 0 & 1\end{pmatrix},$$

where $\mathbb{M}(z)$ is the *modified period map*. Let us write the entries of $\mathbb{M}(z)$ in the following form:

$$\mathbb{M}_{11}(z)=+\sum c^{11}_{\sigma_2,\ldots,\sigma_m}\cos((\mu_1+\sigma_2\mu_2+\cdots+\sigma_m\mu_m)z), \tag{4.8a}$$

$$\mathbb{M}_{12}(z)=+\sum c^{12}_{\sigma_2,\ldots,\sigma_m}\sin((\mu_1+\sigma_2\mu_2+\cdots+\sigma_m\mu_m)z), \tag{4.8b}$$

$$\mathbb{M}_{21}(z)=-\sum c^{21}_{\sigma_2,\ldots,\sigma_m}\sin((\mu_1+\sigma_2\mu_2+\cdots+\sigma_m\mu_m)z), \tag{4.8c}$$

$$\mathbb{M}_{22}(z)=+\sum c^{22}_{\sigma_2,\ldots,\sigma_m}\cos((\mu_1+\sigma_2\mu_2+\cdots+\sigma_m\mu_m)z), \tag{4.8d}$$

where we sum over all sign patterns $(\sigma_2,\ldots,\sigma_m)$ in the 2^{m-1} element set $\{-1,+1\}^{m-1}$. Then the Fourier spectrum of the entries of the modified period map $\mathbb{M}(z)$ is given by

$$\left\{\sum_{j=1}^{m}\sigma_jn_ja_j:\sigma_j=\pm1\right\}.$$

Therefore it has at most 2^m points and its maximum is $\mu_1+\cdots+\mu_m$. Using the addition formulas of trigonometry, we get the recurrence relations

$$c^{11}_{\sigma_2,\ldots,\sigma_{m-1},\pm1}=\frac{1}{2}c^{11}_{\sigma_2,\ldots,\sigma_{m-1}}\pm\frac{1}{2n_m}c^{21}_{\sigma_2,\ldots,\sigma_{m-1}},$$
$$c^{22}_{\sigma_2,\ldots,\sigma_{m-1},\pm1}=\frac{1}{2}c^{22}_{\sigma_2,\ldots,\sigma_{m-1}}\pm\frac{1}{2}n_mc^{12}_{\sigma_2,\ldots,\sigma_{m-1}},$$
$$c^{12}_{\sigma_2,\ldots,\sigma_{m-1},\pm1}=\frac{1}{2}c^{12}_{\sigma_2,\ldots,\sigma_{m-1}}\pm\frac{1}{2n_m}c^{22}_{\sigma_2,\ldots,\sigma_{m-1}},$$
$$c^{21}_{\sigma_2,\ldots,\sigma_{m-1},\pm1}=\frac{1}{2}c^{21}_{\sigma_2,\ldots,\sigma_{m-1}}\pm\frac{1}{2}n_mc^{11}_{\sigma_2,\ldots,\sigma_{m-1}}.$$

We thus easily recover the expression

$$\boldsymbol{c}_{1,\ldots,1}\overset{\text{def}}{=}\begin{pmatrix}c^{11}_{1,\ldots,1} & c^{12}_{1,\ldots,1}\\ c^{21}_{1,\ldots,1} & c^{22}_{1,\ldots,1}\end{pmatrix}=\frac{1}{2^{m-1}}\begin{pmatrix}1 & 1/n_m\\ n_m & 1\end{pmatrix}\cdots\begin{pmatrix}1 & 1/n_1\\ n_1 & 1\end{pmatrix}, \tag{4.9}$$

where the subscript $1,\dots,1$ have $m-1$ entries and the product matrix has positive entries but zero determinant. More generally,

$$\boldsymbol{c}_{\sigma_2,\dots,\sigma_m} \stackrel{\text{def}}{=} \begin{pmatrix} c^{11}_{\sigma_2,\dots,\sigma_m} & c^{12}_{\sigma_2,\dots,\sigma_m} \\ c^{21}_{\sigma_2,\dots,\sigma_m} & c^{22}_{\sigma_2,\dots,\sigma_m} \end{pmatrix} = \frac{1}{2^{m-1}} \begin{pmatrix} 1 & \frac{\sigma_m}{n_m} \\ \sigma_m n_m & 1 \end{pmatrix} \cdots \begin{pmatrix} 1 & \frac{\sigma_2}{n_2} \\ \sigma_2 n_2 & 1 \end{pmatrix} \begin{pmatrix} 1 & \frac{1}{n_1} \\ n_1 & 1 \end{pmatrix}. \quad (4.10)$$

By induction on the number of factors we thus easily prove that

$$\frac{c^{11}_{\sigma_2,\dots,\sigma_m}}{c^{12}_{\sigma_2,\dots,\sigma_m}} = \frac{c^{21}_{\sigma_2,\dots,\sigma_m}}{c^{22}_{\sigma_2,\dots,\sigma_m}} = n_1, \qquad \frac{c^{21}_{\sigma_2,\dots,\sigma_m}}{c^{11}_{\sigma_2,\dots,\sigma_m}} = \frac{c^{22}_{\sigma_2,\dots,\sigma_m}}{c^{12}_{\sigma_2,\dots,\sigma_m}} = \sigma_m n_m. \quad (4.11)$$

4.1. Recovery of the refractive index

In this subsection we propose a method to determine the refractive indices n_j and the layer amplitudes a_j from the modified period map $\mathbb{M}(\eta)$ in the piecewise constant case. This kind of heterostructure generally consists of no more than three layers per period [9,26]. An example of such a periodic structure is depicted in Fig. 2.

4.1.1. Two-layer photonic crystals

Let us consider a crystal where in each period there are two different media with refractive indices n_1 and n_2, respectively, where $n_1 \neq n_2$ (Fig. 4).

- We start from the modified period map $\mathbb{M}_2(z)$ and focus on its Fourier spectrum. For a two-layer photonic crystal its Fourier spectrum will be the 2^2 element set
$$\{\pm(\mu_1+\mu_2), \pm(\mu_1-\mu_2)\} = \{\tilde{\mu}_1, \tilde{\mu}_2, \tilde{\mu}_3, \tilde{\mu}_4\}.$$

- We then consider the maximum of the Fourier spectrum:
$$\tilde{\mu}_i = n_1 a_1 + n_2 a_2 = \mu_1 + \mu_2, \quad (4.12)$$
for some $i \in \{1,2,3,4\}$.

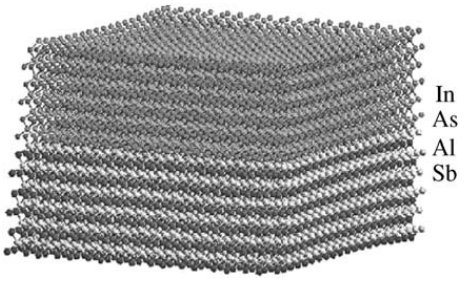

Fig. 4. Example of a heterostructure made of two semiconductor crystals InAs–AlSb with different refractive indices.

- Let $\boldsymbol{c}_+$ be the corresponding coefficient matrix. We evaluate n_1 and n_2 from Eqs. (4.11):
$$\frac{c^{11}_+}{c^{12}_+} = \frac{c^{21}_+}{c^{22}_+} = n_1, \quad \frac{c^{21}_+}{c^{11}_+} = \frac{c^{22}_+}{c^{12}_+} = n_2. \quad (4.13)$$

- We consider the following system:
$$\begin{cases} \mu_1 + \mu_2 = \tilde{\mu}_i, \\ \mu_1 - \mu_2 = \tilde{\mu}_j \end{cases}$$
for any $j \in \{1,2,3,4\}$ *different from* i, so that we get
$$\mu_2^{(j)} = \frac{\tilde{\mu}_i - \tilde{\mu}_j}{2}, \quad j \neq i. \quad (4.14)$$

- For any computed $\mu_2^{(j)}$ (for a two-layer photonic crystal there are three of them), we calculate the reduced modified period map $\mathbb{M}_1^{(j)}(z)$ corresponding to the virtual one-layer photonic crystal
$$\mathbb{M}_1^{(j)}(z) = \begin{pmatrix} \cos(\mu_2^{(j)} z) & -\dfrac{\sin(\mu_2^{(j)} z)}{n_2} \\ n_2 \sin(\mu_2^{(j)} z) & \cos(\mu_2^{(j)} z) \end{pmatrix} \mathbb{M}_2(z). \quad (4.15)$$

- We select the period map which has a corresponding two-element Fourier spectrum (which is consistent with the one-layer virtual photonic crystal) and whose corresponding coefficient matrix satisfies the following relations:
$$\frac{c^{11}}{c^{12}} = \frac{c^{21}}{c^{22}} = n_1, \quad \frac{c^{21}}{c^{11}} = \frac{c^{22}}{c^{12}}. \quad (4.16)$$
Such a period map turns out to be unique and consequently we find the correct $q \stackrel{\text{def}}{=} \mu_2^{(j)}$, which corresponds to the uniquely found $\mathbb{M}_1^{(j)}(z)$.
- We compute $a_2 = q/n_2$ and finally we get the value of a_1 from Eq. (4.12).

Alternatively one can compute a_2 using the crystal period knowledge (see Eq. (4.6)) and realizing that $a_1 + a_2 = p$.

Example 4.1. Consider

$$n_1 = 1, \quad n_2 = 0.5, \quad a_1 = 1, \quad a_2 = 3.$$

Then $\mu_1 = 1$, $\mu_2 = 1.5$ and using Eqs. (4.8a)–(4.8d) and (4.10), it is straightforward to build the corresponding modified period map:

$$\mathbb{M}_{11}(z) = +\tfrac{1}{2}[3\cos(2.5z) - \cos(0.5z)],$$
$$\mathbb{M}_{12}(z) = +\tfrac{1}{2}[3\sin(2.5z) + \sin(0.5z)],$$
$$\mathbb{M}_{21}(z) = -\tfrac{1}{2}[1.5\sin(2.5z) - 0.5\sin(0.5z)],$$
$$\mathbb{M}_{22}(z) = +\tfrac{1}{2}[1.5\cos(2.5z) + 0.5\cos(0.5z)].$$

The coefficient matrices correspond to the Fourier spectrum as follows:

$$+2.5\mapsto\frac{1}{2}\begin{pmatrix}3 & 3\\ 1.5 & 1.5\end{pmatrix},\quad -2.5\mapsto\frac{1}{2}\begin{pmatrix}3 & -3\\ -1.5 & 1.5\end{pmatrix},$$
$$+0.5\mapsto\frac{1}{2}\begin{pmatrix}-1 & 1\\ -0.5 & 0.5\end{pmatrix},\quad -0.5\mapsto\frac{1}{2}\begin{pmatrix}-1 & -1\\ 0.5 & 0.5\end{pmatrix},$$

where $(\mu_1+\sigma_2\mu_2)\mapsto \boldsymbol{c}_{\sigma_2}$. We now perform the inversion:

- find the Fourier spectrum: $\{0.5,-0.5,2.5,-2.5\}$;
- focus on its maximum: $\tilde{\mu}_2=2.5$;
- evaluate

$$n_1=\frac{c_+^{11}}{c_+^{12}}=\frac{c_+^{21}}{c_+^{22}}=1,\quad n_2=\frac{c_+^{21}}{c_+^{11}}=\frac{c_+^{22}}{c_+^{21}}=0.5;$$

- compute $\tilde{\mu}_2^j$ for $j=1,2,4$:

$$\tilde{\mu}_2^1=1,\quad \tilde{\mu}_2^2=1.5,\quad \tilde{\mu}_2^4=2.5;$$

- we calculate $\mathbb{M}_1^{(j)}(z)$ for $j=1,2,4$:

$$[\mathbb{M}_1^{(j)}]_{11}(z)=6\cos[(\tilde{\mu}_2^j-2.5)z]-2\cos[(\tilde{\mu}_2^j-0.5)z],$$
$$[\mathbb{M}_1^{(j)}]_{12}(z)=-6\sin[(\tilde{\mu}_2^j-2.5)z]-2\sin[(\tilde{\mu}_2^j-0.5)z],$$
$$[\mathbb{M}_1^{(j)}]_{21}(z)=3\sin[(\tilde{\mu}_2^j-2.5)z]-\sin[(\tilde{\mu}_2^j-0.5)z],$$
$$[\mathbb{M}_1^{(j)}]_{22}(z)=3\cos[(\tilde{\mu}_2^j-2.5)z]+\cos[(\tilde{\mu}_2^j-0.5)z],$$

and it is easy to show that only for $j=2$ one gets a one-layer modified period map with a two-point Fourier spectrum and for which relations (4.16) are satisfied:

$$\mathbb{M}_1^{(j=2)}(z)=4\begin{pmatrix}\cos z & \sin z\\ -\sin z & \cos z\end{pmatrix};$$

- get $a_2=\tilde{\mu}_2^2/n_2=q/n_2=1.5/0.5=3$ and from $\mathbb{M}_1^{(j=2)}(z)$ realize that $\mu_1=1$;
- finally, obtain a_1 either from $\mu_1+q=\tilde{\mu}_2$ or from $a_1+a_2=\lim_{z\to 0}M^{12}(z)=p$ (see Eq. (4.6)) and find $a_1=1$. Alternatively one gets a_1 straight from μ_1 using the known n_1 value.

4.1.2. General case

The inversion procedure used for the two-layer photonic crystal in Section 4.1.1 can easily be generalized to a photonic crystal made of m layers. In fact, we present the following algorithm.

1. Consider the 2^m-element Fourier spectrum corresponding to the modified period map $\mathbb{M}_m(z)$,

$$\left\{\sum_{j=1}^m\sigma_j\mu_j:\sigma_j=\pm1\right\}=\{\tilde{\mu}_1,\tilde{\mu}_2,\ldots,\tilde{\mu}_{2^m}\},$$

where $\mu_j=n_ja_j$, and find its maximum

$$\tilde{\mu}_i=\mu_1+\mu_2+\cdots+\mu_m,$$

where $i\in\{1,2,\ldots,2^m\}$.

2. Evaluate n_1 and n_m from Eq. (4.11):

$$\frac{c_{+,\ldots,+}^{11}}{c_{+,\ldots,+}^{12}}=\frac{c_{+,\ldots+}^{21}}{c_{+,\ldots+}^{22}}=n_1,\quad \frac{c_{+,\ldots,+}^{21}}{c_{+,\ldots,+}^{11}}=\frac{c_{+,\ldots,+}^{22}}{c_{+,\ldots,+}^{12}}=n_m. \tag{4.17}$$

3. Consider the following system:

$$\begin{cases}\mu_1+\ldots+\mu_{m-1}+\mu_m=\tilde{\mu}_i,\\ \mu_1+\ldots+\mu_{m-1}-\mu_m=\tilde{\mu}_j\end{cases}$$

for any $j\in\{1,2,\ldots i-1,i+1,\ldots,2^m\}$ so that

$$\mu_m^{(j)}=\frac{\tilde{\mu}_i-\tilde{\mu}_j}{2},\quad j\neq i. \tag{4.18}$$

4. For any computed $\mu_m^{(j)}$, calculate the reduced modified period map $\mathbb{M}_{m-1}^{(j)}(z)$:

$$\mathbb{M}_{m-1}^{(j)}(z)=\begin{pmatrix}\cos(\mu_m^{(j)}z) & -\dfrac{\sin(\mu_m^{(j)}z)}{n_m}\\ n_m\sin(\mu_m^{(j)}z) & \cos(\mu_m^{(j)}z)\end{pmatrix}\mathbb{M}(z). \tag{4.19}$$

5. Select the reduced period map whose corresponding spectrum has 2^{m-1} elements and whose coefficient matrix satisfies the following conditions:

$$\frac{c_{m-1}^{11}}{c_{m-1}^{12}}=\frac{c_{m-1}^{21}}{c_{m-1}^{22}}=n_1,\quad \frac{c_{m-1}^{21}}{c_{m-1}^{11}}=\frac{c_{m-1}^{22}}{c_{m-1}^{12}}. \tag{4.20}$$

6. This modified period map turns out to be unique and consequently

$$a_m=\frac{q_m}{n_m},$$

where q_m is the frequency $\mu_m^{(j)}$ corresponding to the unique $\mathbb{M}_{m-1}^{(j)}(z)$ computed at step 5.

7. Repeat the same procedure for $\mathbb{M}_{m-1}(z)$ until the original modified period map has been factorized completely.

After step 3 one can reduce the number of $\mu_m^{(j)}$ by noticing that

$$\boldsymbol{c}_{(1,\ldots,1,1)}+\boldsymbol{c}_{(1,\ldots,1,-1)}=\boldsymbol{C}_{m-1}, \tag{4.21a}$$

$$\boldsymbol{c}_{(1,\ldots,1,1)}-\boldsymbol{c}_{(1,\ldots,1,-1)}=\begin{pmatrix}0 & \dfrac{1}{n_m}\\ n_m & 0\end{pmatrix}\boldsymbol{C}_{m-1}, \tag{4.21b}$$

where $\boldsymbol{C}_{m-1}$ is the leading coefficient matrix [i.e., $\boldsymbol{c}_{(1,\ldots,1)}$] in the modified period map $\mathbb{M}_{m-1}^{(j)}(z)$ for the first $m-1$ intervals. Eqs. (4.21a) and (4.21b) thus reduce the number of available $\mu_m^{(j)}$ so that step 4 is more easily performed.

5. Impurity period map and scattering matrix

Let us now consider a one-dimensional photonic crystal, where the translational symmetry has been broken by the introduction of a localized defect. Such a crystal is depicted in Fig. 5, where the refractive index profile along the x-direction is drawn. To treat it mathematically, we consider the refractive index $n(x)$

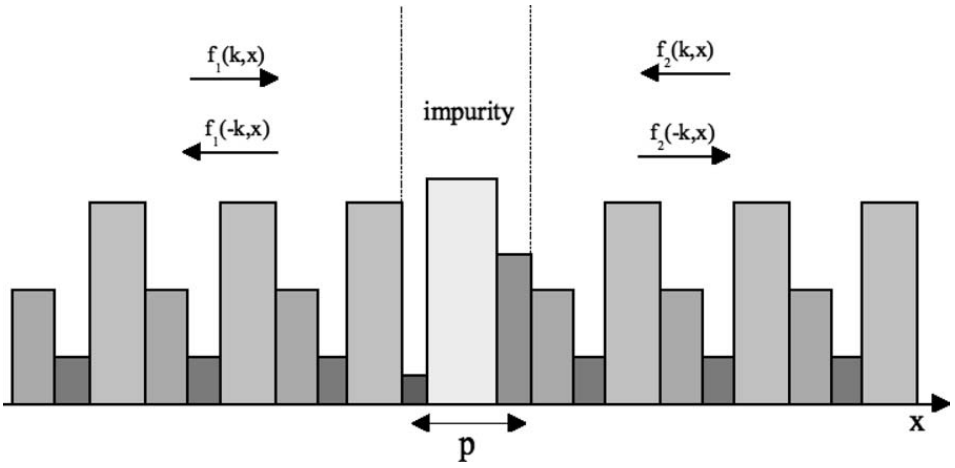

Fig. 5. Example of a periodic structure with period p having a localized impurity due to the presence of materials with different refractive index. The impurity generates scattering phenomena (Jost functions). The refractive index profile along the x-direction is drawn.

with a periodic component and a component describing the effect of impurities. In this case Eq. (2.11) generalizes to

$$\psi''(\eta,x) = -\eta n(x)^2[1+\varepsilon(x)]\psi(\eta,x), \tag{5.1}$$

where $n(x)$ is assumed to be a real piecewise continuous periodic function of period p, $\varepsilon(x)$ is piecewise continuous and vanishes as $x \to \pm\infty$ and $\varepsilon(x) > -1+\delta$ for $\delta > 0$.

The scattering theory of the periodic-plus-impurity Schrödinger equation relevant to the mathematical description of one-dimensional solid and semiconductor crystals is well developed [25]. Apart from the asymptotic theory for large $|\eta|$, the scattering theory for the periodic-times-impurity Helmholtz equation (5.1) can be developed along the same lines. In this article we give a summary of such a theory before applying it to the recovery of the period map from the scattering data. Some of the details are given in [24].

The scattering theory for the periodic-times-impurity Helmholtz equation (5.1) is quite analogous to the scattering theory of the Schrödinger equation on the line [27], where the role of the Floquet solutions to be defined by (5.2) is played by the plane waves e^{ikx} and e^{-ikx}. The analogy is all the more striking if we use the quasimomentum k as a spectral parameter instead of η, which has the effect of converting the combined upper and lower edges of the bands (in η) into the real line (in k) and to convert the complex η-plane outside the bands into the so-called physical upper half complex k-plane. This analogy has led Firsova [25] to develop a scattering theory for the periodic-plus-impurity Schrödinger equation.

5.1. Floquet and Jost functions

Asymptotically Eq. (5.1) admits two linearly independent solutions which play the physical role of plane waves [21–23]. For each non-real η these so-called *Floquet solutions* have the following form:

$$\psi_1(\eta,x) = \theta(\eta,x) + m_1(\eta)\varphi(\eta,x), \tag{5.2a}$$

$$\psi_2(\eta,x) = \theta(\eta,x) + m_2(\eta)\varphi(\eta,x), \tag{5.2b}$$

where $m_{1,2}(\eta)$ are called *Weyl coefficients* and $\theta(\eta,x)$ and $\varphi(\eta,x)$ are the elementary solutions of (2.11) satisfying (3.1). The Weyl coefficients can be calculated by considering the Born–Von Kármán conditions, implying that

$$\begin{pmatrix} \tau_{1,2}(\eta)-\theta(\eta,p) & -\varphi(\eta,p) \\ -\theta'(\eta,p) & \tau_{1,2}(\eta)-\varphi'(\eta,p) \end{pmatrix} \begin{pmatrix} 1 \\ m_{1,2}(\eta) \end{pmatrix} = \begin{pmatrix} 0 \\ 0 \end{pmatrix}. \tag{5.3}$$

Hence

$$m_{1,2}(\eta) = \frac{\tau_{1,2}(\eta)-\theta(\eta,p)}{\varphi(\eta,p)}, \tag{5.4}$$

where $\tau_{1,2}$ are the roots of Eq. (3.3) for $\eta \in \mathbb{C}\backslash\mathbb{R}$. These Floquet solutions have the Bloch representation

$$\psi_{1,2}(k,x) = e^{\pm iky}\chi_{1,2}(k,x), \tag{5.5}$$

where y is the travel time parameter, k is the quasimomentum related to $\eta \in \mathbb{C}\backslash\mathbb{R}$ through Formula (3.11) and $\chi_{1,2}(k,x+p) \equiv \chi_{1,2}(k,x)$ are periodic. We also get for the Wronskian

$$\begin{aligned} w(k) &\stackrel{\text{def}}{=} W[\psi_1(k,\cdot),\psi_2(k,\cdot)] \\ &= W[\theta(\eta,\cdot)+m_1(\eta)\varphi(\eta,\cdot),\theta(k,\cdot)+m_2(\eta)\varphi(k,\cdot)] \\ &= \{m_2(\eta)-m_1(\eta)\}W[\theta(\eta,\cdot),\varphi(\eta,\cdot)] \\ &= m_2(\eta)-m_1(\eta). \end{aligned}$$

Following [25], let us now define the *Jost functions* as those solutions to Eq. (5.1) that satisfy the asymptotic relations (Fig. 5)

$$f_1(k,x) = \psi_1(k,x)[1+o(1)], \quad x \to +\infty, \tag{5.6a}$$

$$f_2(k,x) = \psi_2(k,x)[1+o(1)], \quad x \to -\infty. \tag{5.6b}$$

Then the Jost solutions satisfy the asymptotic relations

$$f_1(k,x) = a_1(k)\psi_1(k,x) + b_1(k)\psi_2(k,x) + o(1), \quad x \to -\infty, \tag{5.7a}$$

$$f_2(k,x) = b_2(k)\psi_1(k,x) + a_2(k)\psi_2(k,x) + o(1), \quad x \to +\infty. \tag{5.7b}$$

where [cf. Eqs. (A.3)]

$$a_1(k) = 1 - w(k)^{-1}I_{21}(k), \quad b_1(k) = w(k)^{-1}I_{11}(k),$$
$$b_2(k) = w(k)^{-1}I_{22}(k), \quad a_2(k) = 1 - w(k)^{-1}I_{12}(k)$$

and

$$I_{jk}(k) = \int_{-\infty}^{\infty} [\eta n(t)^2 \varepsilon(t)]\psi_j(k,t) f_l(k,t)\, dt, \quad j,l = 1,2.$$

Considering Eqs. (5.6) and (5.7) we observe that $f_1(k,x)$ is bounded as $x \to -\infty$ if and only if $a_1(k) = 0$. In the same way $f_2(k,x)$ is bounded as $x \to +\infty$ if and only if $a_2(k) = 0$. Thus, the Jost solutions are bounded for the k-values that are zeros of the functions $a_1(k)$ and $a_2(k)$. As in the case of the periodic-plus-impurity Schrödinger equation [25], these k values correspond to the discrete eigenvalues η inserted into the band gaps by impurities. Usually $a_1(k)$, $a_2(k)$, $b_1(k)$ and $b_2(k)$ are referred to as scattering parameters and they satisfy the useful symmetry relations [24]:

$$a_1(k) = a_2(k) \stackrel{\text{def}}{=} a(k), \quad k \in \mathbb{C}, \tag{5.8a}$$

$$b_1(k) = -b_2(-k) \stackrel{\text{def}}{=} b(k), \quad k \in \mathbb{R}, \tag{5.8b}$$

$$b(-k) = \overline{b(k)}, \quad k \in \mathbb{R}, \tag{5.8c}$$

$$|a(k)|^2 - |b(k)|^2 = 1, \quad k \in \mathbb{R}. \tag{5.8d}$$

5.2. Scattering matrix

Following [25], let us consider coefficients $d_{ij}(k)$ $(i,j = 1,2)$ such that

$$f_1(-k,x) = d_{11}(k)f_1(k,x) + d_{12}(k)f_2(k,x), \tag{5.9a}$$

$$f_2(-k,x) = d_{21}(k)f_1(k,x) + d_{22}(k)f_2(k,x). \tag{5.9b}$$

Using the asymptotic expressions (5.6) as $x \to \pm\infty$, we get

$$\psi_1(-k,x) = d_{11}(k)\psi_1(k,x) + d_{12}(k)[-b(-k)\psi_1(k,x) + a(k)\psi_2(k,x)],$$

$$a(-k)\psi_1(-k,x) + b(-k)\psi_2(-k,x) = d_{11}(k)[a(k)\psi_1(k,x) + b(k)\psi_2(k,x)] + d_{12}(k)\psi_2(k,x),$$

$$-b(k)\psi_1(-k,x) + a(-k)\psi_2(-k,x) = d_{21}(k)\psi_1(k,x) + d_{22}(k)[-b(-k)\psi_1(k,x) + a(k)\psi_2(k,x)],$$

$$\psi_2(-k,x) = d_{21}(k)[a(k)\psi_1(k,x) + b(k)\psi_2(k,x)] + d_{22}(k)\psi_2(k,x).$$

Using $\psi_{1,2}(-k,x) = \psi_{2,1}(k,x)$ and the linear independence of the Floquet solutions to equate coefficients of $\psi_1(k,x)$ and $\psi_2(k,x)$ we get

$$0 = d_{11}(k) - d_{12}(k)b(-k), \quad 1 = d_{12}(k)a(k),$$
$$b(-k) = d_{11}(k)a(k), \quad a(-k) = d_{11}(k)b(k) + d_{12}(k),$$
$$a(-k) = d_{21}(k) - d_{22}(k)b(-k), \quad -b(k) = d_{22}(k)a(k),$$
$$1 = d_{21}(k)a(k), \quad 0 = d_{21}(k)b(k) + d_{22}(k).$$

Therefore,

$$\begin{pmatrix} d_{11}(k) & d_{12}(k) \\ d_{21}(k) & d_{22}(k) \end{pmatrix} = \frac{1}{a(k)} \begin{pmatrix} b(-k) & 1 \\ 1 & -b(k) \end{pmatrix}, \quad k \in \mathbb{R}.$$

We now define the *transmission coefficient* $T(k)$, the *reflection coefficient from the right* $R(k)$, and the *reflection coefficient from the left* $L(k)$ by

$$T(k) = d_{12}(k) = d_{21}(k) = \frac{1}{a(k)}, \tag{5.10a}$$

$$R(k) = -d_{11}(k) = -\frac{b(-k)}{a(k)}, \tag{5.10b}$$

$$L(k) = -d_{22}(k) = \frac{b(k)}{a(k)}, \tag{5.10c}$$

where $k \in \mathbb{R}$. Then (5.8d) implies that the *scattering matrix*

$$S(k) = \begin{pmatrix} T(k) & R(k) \\ L(k) & T(k) \end{pmatrix}, \quad k \in \mathbb{R}, \tag{5.11}$$

is unitary. Using formulas (5.8a), (5.8c), (5.8d) and (5.10), it is easily shown that

$$|T(k)|^2 + |R(k)|^2 = |T(k)|^2 + |L(k)|^2 = 1$$

which corresponds to conservation of energy.

5.3. Recovering period map from scattering matrix

In this section we recover the relationship between the period map and the scattering coefficients $a(k)$ and $b(k)$.

Let the impurity be concentrated in the period $(0,p]$ and let us refer to the rest of the crystal by the term *bulk*. Assuming the period $(0,p]$ and the bulk to be piecewise constant, we define

$$n(x)\sqrt{[1+\varepsilon(x)]} = \begin{cases} \widetilde{n}_j, & \widetilde{b}_{j-1} < x \le \widetilde{b}_j,\ j = 1,\dots,l, \\ n(x), & x \notin [0,p], \end{cases}$$

where $0 = \widetilde{b}_0 < \widetilde{b}_1 < \cdots < \widetilde{b}_l = p$ and $n(x)$ is as in Section 4.

Now let us define $M^{imp}(\eta)$ as the matrix $M(\eta)$ of Section 4, but with n_j replaced by $\widetilde{n}_j$ $(j = 1,\dots,l)$. Then outside the interval $[0,p]$ the Jost solutions can be expressed in terms

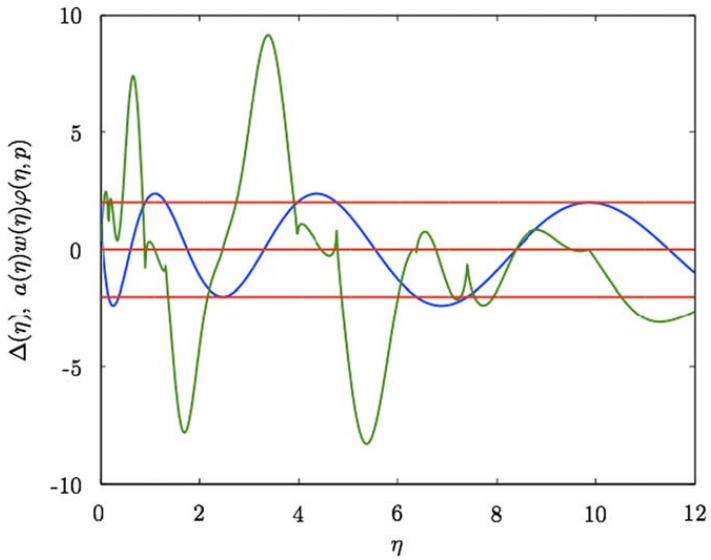

Fig. 6. In this figure the function $\Delta(\eta)$ is drawn in blue, whereas $a(\eta)w(\eta)\varphi(\eta,p)$ is in green. The system considered is a two-layer photonic crystal with $n_1=1$, $n_2=2$, $a_1=2$, $a_2=2$ and $\Delta(\eta)$ has been computed using Eq. (4.5). The impurity is thought concentrated in one period of length $p=4$ whose optical properties are parameterized by $n_1^{imp}=2, n_2^{imp}=1, a_1^{imp}=3$ and $a_2^{imp}=0.9$, while $a(\eta)w(\eta)\varphi(\eta,p)$ has been calculated by making use of Eq. (5.15). (For interpretation of the references to color in this figure legend, the reader is referred to the web version of this article.)

of the Floquet solutions as follows (see Eqs. (5.7) and (5.10)):

$$f_1(k,x)=\begin{cases}\psi_1(k,x), & x\geq p,\\ a(k)\psi_1(k,x)+b(k)\psi_2(k,x), & x\leq 0,\end{cases}$$

$$f_2(k,x)=\begin{cases}-\overline{b(\bar{k})}\psi_1(k,x)+a(k)\psi_2(k,x), & x\geq p,\\ \psi_2(k,x), & x\leq 0.\end{cases}$$

Putting

$$W(k,x)\stackrel{\text{def}}{=}\begin{pmatrix}\psi_1(k,x) & \psi_2(k,x)\\ \psi_1'(k,x) & \psi_2'(k,x)\end{pmatrix}, \tag{5.12}$$

we obtain

$$\begin{aligned}W(k,0)\begin{pmatrix}a(k)\\ b(k)\end{pmatrix}&=\begin{pmatrix}f_1(k,0)\\ f_1'(k,0)\end{pmatrix}=M^{imp}(\eta)^{-1}\begin{pmatrix}f_1(k,p)\\ f_1'(k,p)\end{pmatrix}\\ &=M^{imp}(\eta)^{-1}\begin{pmatrix}\psi_1(k,p)\\ \psi_1'(k,p)\end{pmatrix}\\ &=M^{imp}(\eta)^{-1}M(\eta)\begin{pmatrix}\psi_1(k,0)\\ \psi_1'(k,0)\end{pmatrix}\end{aligned}$$

and

$$\begin{aligned}W(k,0)\begin{pmatrix}-\overline{b(\bar{k})}\\ a(k)\end{pmatrix}&=M(\eta)^{-1}W(k,p)\begin{pmatrix}-\overline{b(\bar{k})}\\ a(k)\end{pmatrix}\\ &=M(\eta)^{-1}\begin{pmatrix}f_2(k,p)\\ f_2'(k,p)\end{pmatrix}\\ &=M(\eta)^{-1}M^{imp}(\eta)\begin{pmatrix}f_2(k,0)\\ f_2'(k,0)\end{pmatrix}\\ &=M(\eta)^{-1}M^{imp}(\eta)\begin{pmatrix}\psi_2(k,0)\\ \psi_2'(k,0)\end{pmatrix}.\end{aligned}$$

As a result of $w(k)=m_2(\eta)-m_1(\eta)$, $\psi_1(k,0)=\psi_2(k,0)=1$, $\psi_1'(k,0)=m_1(\eta)$, and $\psi_2'(k,0)=m_2(\eta)$ we get

$$\begin{pmatrix}a(k)\\ b(k)\end{pmatrix}=\frac{1}{w(k)}\begin{pmatrix}m_2(\eta) & -1\\ -m_1(\eta) & 1\end{pmatrix}M^{imp}(\eta)^{-1}M(\eta)\begin{pmatrix}1\\ m_1(\eta)\end{pmatrix}, \tag{5.13a}$$

$$\begin{pmatrix}-\overline{b(\bar{k})}\\ a(k)\end{pmatrix}=\frac{1}{w(k)}\begin{pmatrix}m_2(\eta) & -1\\ -m_1(\eta) & 1\end{pmatrix}M^{imp}(\eta)M(\eta)^{-1}\begin{pmatrix}1\\ m_2(\eta)\end{pmatrix}. \tag{5.13b}$$

Eqs. (5.13)allow us to compute the period map $M^{imp}(\eta)$ of the periodic plus impurity problem if the impurity is concentrated in one period. The latter scattering data can easily be computed from one reflection coefficient and the transmission coefficient by using (5.8d) and (5.10). Let us now write $N(\eta)=M^{imp}(\eta)^{-1}M(\eta)$. Then

$$\begin{aligned}a(\eta)=\frac{1}{w(\eta)}\Big\{&[m_2(\eta)+m_1(\eta)]\frac{1}{2}[N_{11}(\eta)-N_{22}(\eta)]-N_{21}(\eta)\\ &+m_2(\eta)m_1(\eta)N_{12}(\eta)\\ &+[m_2(\eta)-m_1(\eta)]\frac{1}{2}[N_{11}(\eta)+N_{22}(\eta)]\Big\}.\end{aligned} \tag{5.14}$$

Now for $\Delta(\eta)\notin[-2,2]$ we have

$$w(\eta)=m_2(\eta)-m_1(\eta)=\frac{\tau_2(\eta)-\tau_1(\eta)}{\varphi(\eta,p)},$$

$$m_2(\eta)+m_1(\eta)=\frac{\Delta(\eta)-2\theta(\eta,p)}{\varphi(\eta,p)}=\frac{\varphi'(\eta,p)-\theta(\eta,p)}{\varphi(\eta,p)},$$

$$m_2(\eta)m_1(\eta) = \frac{\tau_2(\eta)\tau_1(\eta) - [\tau_2(\eta)+\tau_1(\eta)]\theta(\eta,p) + \theta(\eta,p)^2}{\varphi(\eta,p)^2} = \frac{1 - [\theta(\eta,p)+\varphi'(\eta,p)]\theta(\eta,p) + \theta(\eta,p)^2}{\varphi(\eta,p)^2} = -\frac{\theta'(\eta,p)}{\varphi(\eta,p)}.$$

Consequently,

$$\begin{aligned} &a(\eta)w(\eta)\varphi(\eta,p) \\ &\quad = \tfrac{1}{2}[N_{11}(\eta)+N_{22}(\eta)]w(\eta)\varphi(\eta,p) - N_{21}(\eta)\varphi(\eta,p) \\ &\qquad + \tfrac{1}{2}[N_{11}(\eta)-N_{22}(\eta)][\varphi'(\eta,p)-\theta(\eta,p)] \\ &\qquad - N_{12}(\eta)\theta'(\eta,p). \end{aligned} \tag{5.15}$$

It can be shown [24] that $w(\eta)\varphi(\eta,p) = \sqrt{\Delta(\eta)^2-4}$ and therefore looking for the zeros of $a(\eta)$ amounts to searching for the roots of $a(\eta)w(\eta)\varphi(\eta,p)$, because $\Delta(\eta)\notin[-2,2]$. Consequently, Eq. (5.15) presents a way to find the discrete eigenvalues in a band gap of a one-dimensional photonic crystal (Fig. 6).

6. Conclusions

In this paper the fundamental properties of one-dimensional photonic crystals have been described from the theoretical point of view. First, we derived from Maxwell's equations the eigenvalue problem to study propagation of TEM modes, then we introduced the period map and presented an analytical way to compute the photonic crystal band structure. We analyzed a structure consisting of a finite number of periodic layers with constant refractive index (piecewise constant case), and developed an algorithm to recover the index of refraction when each period of the lattice consists of an arbitrary number of different materials. Finally, we paid attention to a crystal with a localized impurity and estimated the resulting discrete eigenvalues in band gaps by introducing the impurity period map in the piecewise constant case and relating it to the scattering coefficients $a(k)$ and $b(k)$.

Although mono-dimensional photonic crystals are useful to confine radiation and realize laser Fabry–Perot cavities, bi- and tri-dimensional photonic crystals may be employed to develop a wide range of high performance optical devices. In this context, a profound mathematical analysis is a key point. A one-dimensional analytical approach is essential to have sufficient insight in order to understand how to generalize to higher dimensions. For example, it would be very useful to be able to extend the Hill discriminant method to two and three-dimensional cases, i.e., to get the crystal band structure by making the trace of a *generalized* period map to be a bounded set. An inversion procedure in the multi-dimensional case would allow us to design photonic crystals with customized forbidden frequency regions.

Appendix A. Some integral relations

In this appendix we state some integral relations needed to derive (5.6). We assume that $n(x)$ is a positive, piecewise constant, and periodic function of period p. For details we refer to [24].

The following result is easily derived by the method of variation of parameters:

Let $g(x)$ be a bounded measurable function. Then the unique solutions of the inhomogeneous differential equation

$$-\psi''(\eta,x) = \eta n(x)^2\psi(\eta,x) + g(x) \tag{A.1}$$

satisfying $\psi(k,x) = \psi_{1,2}(k,x)[1+o(1)]$ as $x\to\pm\infty$ are given by

$$\psi(\eta,x) = \psi_1(k,x) + \int_x^\infty \frac{\psi_2(k,x)\psi_1(k,t)-\psi_1(k,x)\psi_2(k,t)}{w(k)} g(t)\,dt, \tag{A.2a}$$

$$;\ \psi(\eta,x) = \psi_2(k,x) - \int_{-\infty}^x \frac{\psi_2(k,x)\psi_1(k,t)-\psi_1(k,x)\psi_2(k,t)}{w(k)} g(t)\,dt, \tag{A.2b}$$

respectively.

For $g = [\eta n^2\varepsilon]f_{1,2}(\eta,\cdot)$ we get

$$f_1(k,x) = \psi_1(k,x) + \int_x^\infty A(k;x,t)[\eta n(t)^2\varepsilon(t)]f_1(k,t)\,dt, \tag{A.3a}$$

$$f_2(k,x) = \psi_2(k,x) - \int_{-\infty}^x A(k;x,t)[\eta n(t)^2\varepsilon(t)]f_2(k,t)\,dt, \tag{A.3b}$$

where

$$A(k;x,t) = \frac{\psi_2(k,x)\psi_1(k,t)-\psi_1(k,x)\psi_2(k,t)}{w(k)}. \tag{A.4}$$

References

[1] Diatoms and Photonic Crystals: ⟨http://www.viewsfromscience.com/⟩.
[2] Wickham S, Large M, Poladian L, Jermiin L. Exaggeration and suppression of iridescence: the evolution of two-dimensional butterfly structural colours. J R Soc Interface 2006;3(6):99–108.
[3] Kosaka H, Kawashima T, Tomita A, Notomi M, Tamamura T, Sato T, et al. Superprism phenomena in photonic crystals: toward microscalelightwave circuits. J Lightwave Technol 1999;17:2032–8.
[4] Joannopoulos JD, Meade RD, Winn JN. Photonic crystals, molding the flow of light. Princeton: Princeton University Press; 2006.
[5] Sakoda K. Optical properties of photonic crystals. New York: Springer; 2001.
[6] Broeng J, Mogilevstev D, Barkou SE, Bjarklev A. Photonic crystal fibers: a new class of optical waveguides. Opt Fiber Technol 1999;5:305–30.
[7] CRYSTAL FIBRE: ⟨http://www.crystal-fibre.com/⟩.
[8] De La Rue R, Chong H, Gnan M, Johnson N, Ntakis I, Pottier P, et al. Photonic crystal and photonic wire nano-photonics based on silicon-on-insulator. New J Phys 2006;8.
[9] Istrate E, Sargent EH. Photonic crystal heterostructures and interfaces. Rev Mod Phys 2006;78:455–81.
[10] Giorgio A, Pasqua D, Gina Perri A. Cristalli fotonici: principi di funzionamento ed applicazioni—prima parte, La comunicazione—note, recensioni e notizie, numero unico, 2003. p. 173–85.

[11] Giorgio A, Pasqua D, Gina Perri A. Cristalli fotonici: principi di funzionamento ed applicazioni—seconda parte, La comunicazione—note, recensioni e notizie, numero unico, 2004. p. 165–82.
[12] Momeni B, Huang J, Soltani M, Askari M, Mohammadi S, Rakhshandehroo M, et al. Compact wavelength demultiplexing using focusing negative index photonic crystal superprisms. Opt Exp 2006;14:2413–22.
[13] Fatih Yanik M, Fan S, Soljačić M, Joannopoulos JD. All-optical transistor action with bistable switching in a photonic crystal cross-waveguide geometry. Opt Lett 2003;28(24):2506–8.
[14] Osher SJ, Santosa F. Level set methods for optimization problems involving geometry and constraints. J Comput Phys 2001;171:272–88.
[15] Kao CY, Osher S, Yablonovitch E. Maximizing band gaps in two-dimensional photonic crystals, using level set methods. Appl Phys B 2005;81:235–44.
[16] Yeh P, Yariv A, Hong C-H. Electromagnetic propagation in periodic stratified media. I. General theory. J Opt Soc A 1977;67:423–37.
[17] Yeh P. Optical waves in layered media. New York: Wiley; 1988.
[18] Inoue K, Ohtaka K. Photonic crystals. Physics, fabrication, and applications. Berlin: Springer; 2004.
[19] Nusinsky I, Hardy AA. Band-gap analysis of one-dimensional photonic crystals and conditions for gap closing. Phys Rev B 2006;73:125104.
[20] Nusinsky I, Hardy AA. Erratum: band-gap analysis of one-dimensional photonic crystals and conditions for gap closing. Phys Rev B 2008;77:199901(E).
[21] Magnus W, Winkler S. Hill's equation. New York: Dover Publications; 1979.
[22] Titchmarsh EC. Eigenfunction expansions associated with second-order differential equations, vol. II. Oxford: Clarendon Press; 1958.
[23] Eastham MSP. The spectral theory of periodic differential equations. Edinburgh and London: Scottish Academic Press; 1973.
[24] van der Mee C, Pintus P, Seatzu S. Mathematical principles in photonic crystals. Riv. Mat. dell'Univ. Parma, Ser. 7 2008;8: 99–137.
[25] Firsova NE. Riemann surface of quasimomentum and scattering theory for the perturbed Hill operator. J Math Sci 1979;11(3): 487–97.
[26] Sze SM. Physics of semiconductor devices. 2nd ed. New York: Wiley; 1981.
[27] Faddeev LD. Properties of the *S*-matrix of the one-dimensional Schrödinger equation. Am Math Soc Transl 1964;2:139–66;
Faddeev LD. Properties of the *S*-matrix of the one-dimensional Schrödinger equation. Trudy Mat. Inst. Steklova 1964;73:314–36 [Russian].